Proceedings of the Sixth International Conference on
Railway Technology: Research, Development and Maintenance
Edited by: J. Pombo
Civil-Comp Conferences, Volume 7, Paper 20.5
Civil-Comp Press, Edinburgh, United Kingdom, 2024
ISSN: 2753-3239, doi: 10.4203/ccc.7.20.5

Predicting Failure of Tongue Compression End Fittings

S. M. Barrans[1], M. Newton[2] and C. Greensill[2]

[1]Institute of Railway Research, School of Computing and Engineering, University of Huddersfield
Huddersfield, UK
[2]Product Development, Associated Utility Supplies
Huddersfield, UK

Abstract

A common form of cantilever used to support the overhead line equipment is assembled from steel tubes with crimped in end fittings. Within the older UK stock, these end fittings have been seen to come loose. In this paper, the crimping operation and the pull-out strength of the joint created is determined using finite element analysis (FEA). This analysis demonstrates the reduction in joint strength when sleeve is used to allow a small fitting to be used in a larger diameter tube. A new, machined from solid fitting is proposed and tested. Good correlation between the practical tests and the FEA is observed.

Keywords: overhead line, cantilever, steel tube, crimped connection, finite element analysis, pull out force.

1 Introduction

A very common form of overhead line equipment (OLE) support is the single-track cantilever. Whilst cantilevers have evolved over time, large sections of the UK network use a traditional system formed from galvanized steel tubes and cast-iron fittings. A detailed view of a cast iron tongue compression end fitting, used in this type of cantilever is shown in figure 1.

Failure of components within the cantilever system, or other parts of the OLE can have very serious consequences. In 2012, the Rail Accidents Investigation Board (RAIB) reported [1] on a tramway cantilever that had failed at an insulator and resulted in the tram's pantograph becoming entangled in the OLE. Parts of the OLE

then crashed through the windows of the tram and 3 passengers required hospital treatment. In 2013 the RAIB reported [2] that collision of a pantograph with a cantilever structure had resulted in the pantograph assembly breaking free from the roof of the locomotive and breaking two carriage windows as it fell to the ground. Whilst the root cause of this accident was not cantilever failure, it does emphasise the potential damage that could occur if a cantilever did fail. More recently, a tongue compression end fitting was observed to have come free from the steel tube on a UK1 series cantilever, as shown in figure 2. There is also concern that these assemblies may be corroding internally due to water ingress.

Figure 1: Detailed view of tongue compression end fitting before and after assembly.

Figure 2: Failed tongue compression end fitting to tube connection.

The need to maintain the existing OLE system and the failure of at least one tongue compression assembly has prompted the current study. This aims to gain a more detailed understanding of the components and assembly process and how these influence pull out load in order to guide future product development.

2 Assembling the tongue compression end fitting

Detailed instructions for the assembly of end fittings are provided by NetworkRail [3]. The tongue compression end fitting is manufactured to be a loose fit within the steel tube. If it is found that the inner surface of the tube has weld spatter, excess galvanized coating or a seam ridge preventing insertion of the fitting, the working instruction specifies that the inner diameter be reamed. Once inserted into the tube, a hydraulic press is used to crimp the tube into the recess in the body of the fitting, as shown in figure 3. Each jaw of the crimping tool has three flat faces resulting in six indentations being generated in the tube. The crimping process is a manual operation with pressure being increased until the two faces of the jaws come together. During the crimping process, the flat faces of the end fitting are kept horizontal and therefore perpendicular to the direction of motion of the jaws.

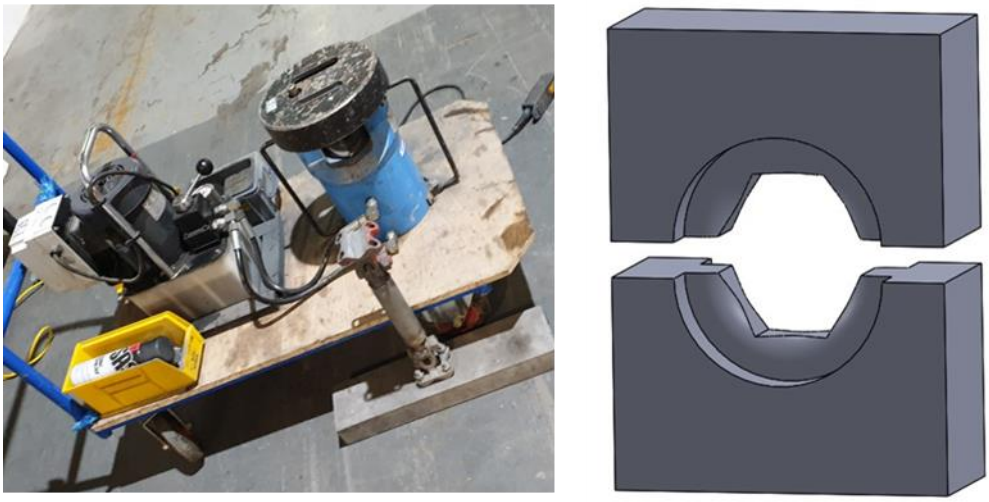

Figure 3: Hydraulic crimping tool and detail of jaws

Within the UK1 series, two sizes of tube may be used for cantilever structures with outer diameters of 48.3 mm and 42.4 mm. Fittings are available with outer diameters to match the inner diameters of the tubes. There is also an approved aluminium sleeve, designed to go over the tail of the smaller fitting, to allow this fitting to be used in the larger tube.

3 Assembly properties

As the tongue compression fitting assembly is being designed as a replacement part within existing cantilever structures, the design is highly constrained: as far as possible it must use existing, approved parts and materials. It must also provide the same performance in terms of pull-out load and should be assembled using the existing crimping machine. The three alternate versions of the assembly are shown in figure 4 with details in table 1. The load requirement shown in table 1 includes a safety factor of 2.5 applied to both tube sizes. The load requirements have been taken from

available drawings of the current fittings [4], [5]. Also shown in table 1 is the range of internal diameters across a sample of 10 for each tube size.

Tube spec	Nominal OD (mm)	Nominal ID (mm)	Minimum ID (mm)	Maximum ID (mm)	Average ID (mm)	Required pull out load (kN)
148/027	48.4	40.4	39.97	40.53	40.25	41.63
148/028	42.4	34.4	34.77	34.89	34.83	22.1

Table 1: Tube sizes and load requirements

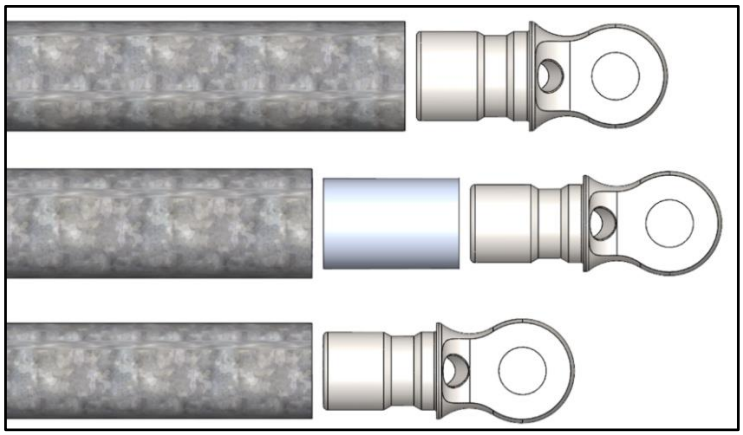

Figure 4: End fitting assembly variants – exploded views. Top: Large fitting in large tube. Middle: Small fitting in large tube with adaptor. Bottom: Small fitting in small tube.

The galvanized steel tubes used in the cantilever assembles are hot finished with the material designation S335J2H in European Standards [6]. Whilst these standards give minimum values for yield strength and elongation along with a nominal value for tensile strength, these values can be exceeded, and the material still be within specification. This can have a significant impact on the plastic deformation of the material. This plastic deformation determines the form of the tube after crimping and therefore has a substantial effect on pull out load. Yun and Gardner [7] have reviewed the behaviour of this class of steel and, based on an extensive range of published experimental data, have proposed a quad linear stress-strain model. For S335J2H, this model can be defined by the data appoints shown in Table 2. A Young's modulus of 210 GPa and Poisson's ratio of 0.3 were used for steel components. This material model will be adapted in the analysis presented in this paper.

	S355		S275	
Point	Stress (MPa)	Strain	Stress (MPa)	Strain
Initial yield	355	1.69×10^{-3}	275	1.31×10^{-3}
Start of strain hardening	355	17.4×10^{-3}	275	15×10^{-3}
End of initial strain hardening	439	54.4×10^{-3}	372	65.3×10^{-3}
Ultimate failure	490	165×10^{-3}	430	216×10^{-3}

Table 2: Steel quad linear material model data points

It was proposed to replace the cast iron end fitting with a fitting machined from structural steel, S275. For the structural steel, a quad linear model was again defined based on Yun and Gardner, as shown in Table 2.

For fittings using the aluminium packing piece, grade 1050A in any condition ranging from H3 to H6 is specified [8]. Again, a bilinear material model was used. The material models for the aluminium bronze and aluminium are shown in table 3. These properties were taken from AZO Materials [9] for the H6 condition.

Young's modulus (GPa)	69
Poisson's ratio	0.33
Initial yield stress (MPa) (0.2% proof stress)	120
Initial yield strain	0.029×10^{-3}
Tensile strength (MPa)	130
Ultimate strain	0.07

Table 3: Material model for aluminium 1050A

3 FEA model

In order to predict the pull-out force for the end fittings, it was necessary to predict the amount of plastic deformation generated during the crimping process. Therefore, the model had to include not only the fitting, tube and aluminium spacer (where applicable) but also the jaws of the crimping tool. This gave the potential for models to become very large. To reduce model size, it was recognized that for the cases of the small fitting in the small tube and the large fitting in the large tube, two planes of symmetry were present. A model of only a quarter of the assembly was generated, as shown in figure 5.

For the assembly including the aluminium adaptor, if it is assumed that the split in the adaptor is on the x-y plane then this plane is still a plane of symmetry. This part is not then symmetric about the y-z plane, indicating that only a single plane of symmetry can be used. However, preliminary studies, comparing models of this assembly with the single plane of symmetry and the two planes of symmetry indicated that ignoring the split in the tube made no significant difference to the pull-out force. Two planes of symmetry were therefore used for all models.

Although the jaws are made from hardened tool steel and should not deform plastically, they will deform elastically. They were therefore given the elastic properties of steel, as used for the end fitting and tube. The pin with which the end fitting interacts may be cast iron or steel, depending on the age of the cantilever assembly. However, the point of interaction is far from the interaction between the end fitting and the tube. Localised deformations due to the interaction will therefore not affect the pull-out force. To reduce model size whilst maintaining model stability, the pin outer surface was modelled as a rigid surface.

As the geometry of the tube, end fitting, adaptor and pin were doubly symmetric and the response of these components was predicted to be doubly symmetric, these parts were constrained so that they could not displace across the planes of symmetry, as indicated in figure 5. For the jaws, symmetry was enforced across the y-z plane.

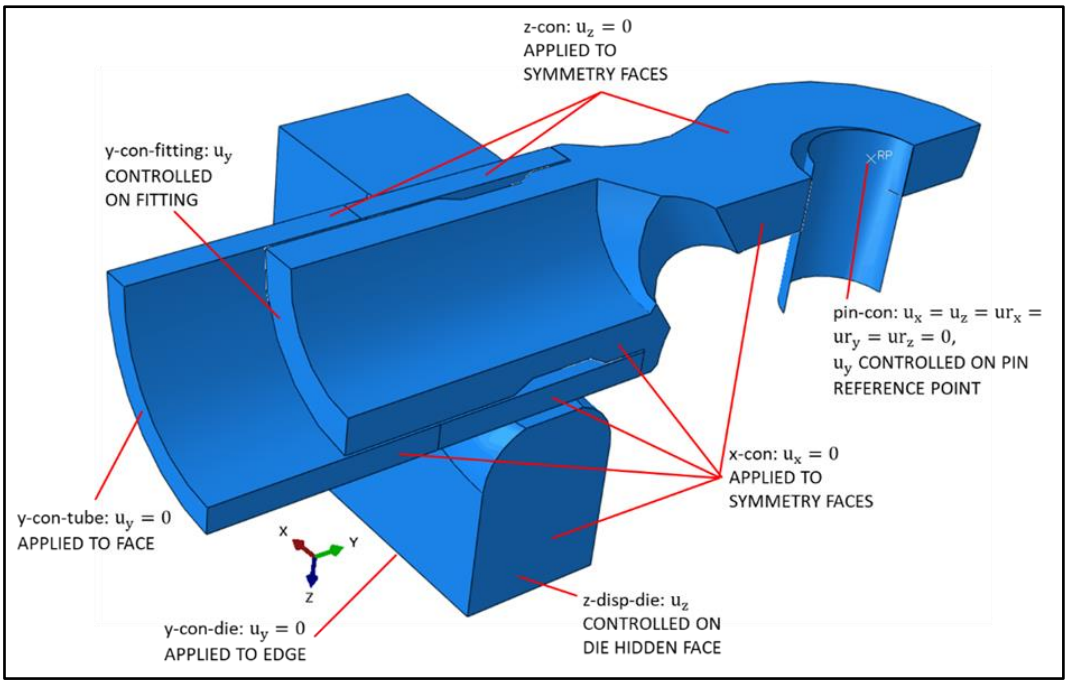

Figure 5: Finite element model geometry and boundary conditions (large fitting in large tube)

The analysis was split into three steps: 'crimp', where the jaws were closed; 'release', where the jaws were retracted and 'pull', where a displacement was applied to the pin. During the crimp and release steps, the fitting and adaptor (where present) were constrained in the y direction. The steps and boundary conditions are summarised in table 4.

BOUNDARY CONDITION	STEP		
	CRIMP	RELEASE	PULL
x-con ($u_x = 0$)	ACTIVE	ACTIVE	ACTIVE
y-con-tube ($u_y = 0$)	ACTIVE	ACTIVE	ACTIVE
y-con-fitting ($u_y = 0$)	ACTIVE	DEACTIVATED	
y-con-die ($u_y = 0$)	ACTIVE	ACTIVE	ACTIVE
z-con ($u_z = 0$)	ACTIVE	ACTIVE	ACTIVE
z-disp-die	$u_z = -3.8$	$u_z = 0.5$	$u_z = 0.5$
pin-con ($u_x = u_z = ur_x = ur_y = ur_z = 0$)	$u_y = 0$	$u_y = 0$	$u_y = 20$

Table 4: Summary of boundary conditions

Contact interactions were defined between the pin and the eye of the fitting and between the jaws and the outer surface of the tube. Where the adaptor was not present, contact was defined between the inner surface of the tube and the outer surface of the fitting. Where the adaptor was present, contact interactions were defined between the inner surface of the tube and the outer surface of the adaptor and between the inner

surface of the adaptor and the outer surface of the fitting. Where motion tangential to the contact direction was likely to occur, a coefficient of friction of 0.1 was specified. This low value was used as these fittings are assembled with a conductive grease.

For the tube and adaptor, hexahedral, linear elements with reduced integration were used, as recommended by Dassault Systemes [10] for problems such as this where the mesh may be highly distorted during deformation and where there is the potential for shear locking within the fully integrated version of the element. To ensure that the plastic deformation was effectively captured, eight elements were used through the wall thickness of the tube and six through the wall thickness of the adaptor, as shown in figure 6. For the fitting and jaws, a fully integrated, quadratic tetrahedral element was specified to allow the complex geometry with curved surfaces to be effectively meshed. Smaller elements were specified in the areas of contact.

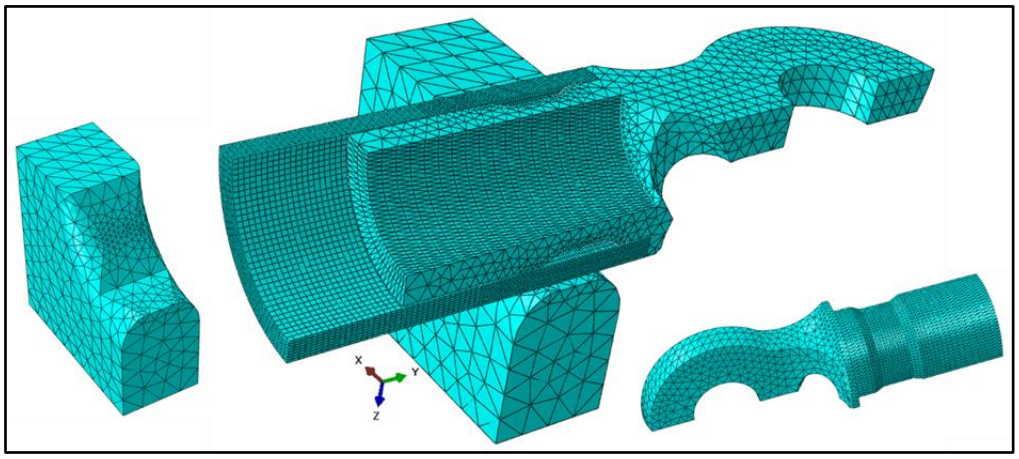

Figure 6: Finite element mesh (large fitting in large tube)

3 Simulation results

Figure 7 shows the radial displacement of the tube (viewed from inside the tube) with the full crimp load applied and with that load removed. The largest radial deformation is seen with the large fitting inside the large tube. The displacement of the smaller tube is 30% less than this. In neither case is the radial deformation sufficient for the tube to touch the bottom of the groove in the outer diameter of the fitting. The displacement seen is therefore principally a function of the geometry of the crimping tool jaws. However, when the adaptor is used to allow the small fitting to be used with the large tube, the adaptor does press against the bottom of the groove and the tube wall is slightly compressed.

As shown in figure 8, high levels of stress are generated during the crimping process ensuring that in all three cases, there is little elastic spring back. This figure shows a partial section of the model, taken midway along the groove in the fitting. Associated with these high stresses are high levels of equivalent plastic strain. These tend to be concentrated towards the centre of the tube wall, on the edge of the crimp contact zone. This indicates that they are genuine plastic strains, due principally to shear forces, rather than being induced by unrealistic contact conditions. Within the

steel tube, the largest areas of plastic strain occur with the large fitting in the large tube. In figure 8A an area of very high equivalent plastic strain is shown in the aluminium adaptor which is crushed between the fitting and the tube at the edge of the groove.

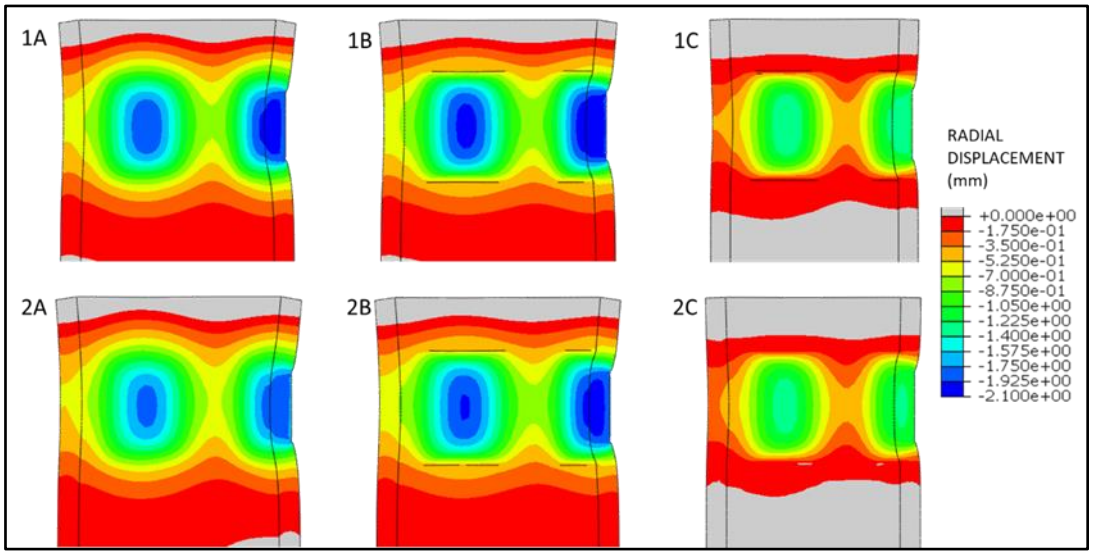

Figure 7: Tube radial displacement. 1: With crimp load applied, 2: With crimp load removed, A: Small fitting in large tube, B: Large fitting in large tube, C: Small fitting in small tube

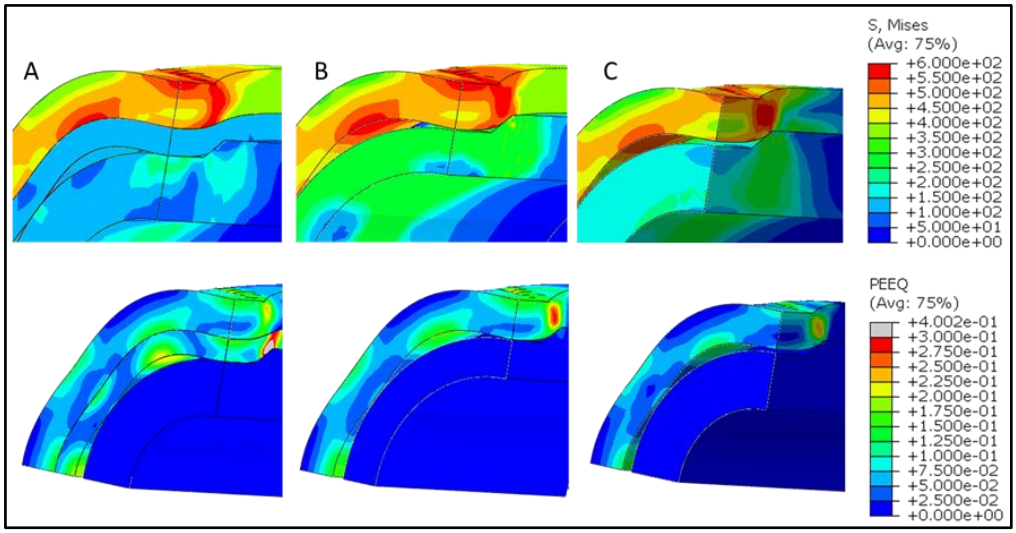

Figure 8: Von Mises stress (MPa) (top), plastic strain (bottom) crimp load applied. A: Small fitting / large tube, B: Large fitting / large tube, C: Small fitting / small tube

In addition to assessing potential material failure during the crimping process, the analysis was also required to predict the end fitting pull out load. This load was monitored using the reaction force at the pin reference point, where displacement was prescribed. Pull out load as a function of pin displacement is shown in figure 9 for the

small fitting in the small tube. The peak pull out force occurs with a small amount of displacement as the back edge of the groove in the fitting impinges against the indentation in the tube generated by crimping. This interference is overcome by the fitting pushing the tube wall out, in the radial direction and the axial force required to move the fitting reduces. A second resistance to pull out occurs when the back of the groove reaches the front of the crimp indentation with the indented tube material being constrained by the undeformed tube material. Once this resistance is overcome, the axial reaction force reduces rapidly with a final, small resistance occurring as the back of the groove moves into the undeformed tube region.

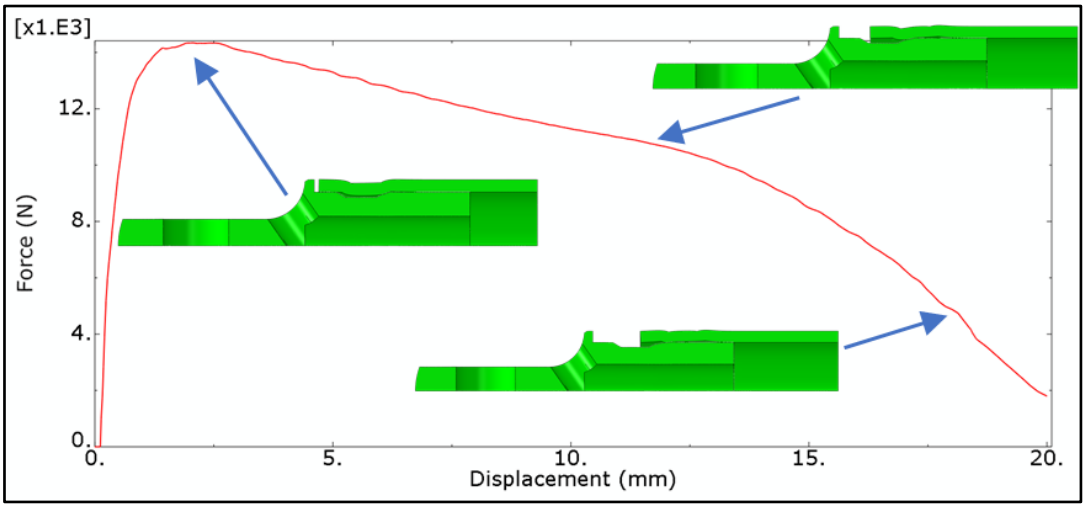

Figure 9: Axial reaction force (small fitting in small tube)

Noting that the models used were a quarter of each assembly, the peak axial reaction force observed must be quadrupled to give the predicted pull-out force. This force is shown in table 5 for each assembly, alongside the requirement taken from table 1. The small fitting in the small tube assembly exceeds the load requirement by a factor of 2.6 and the large fitting – large tube assembly also exceeds the required load by a factor of 1.5. However, assembling the small fitting in the large tube using the aluminium adaptor gives a load capacity which is only 65% of the requirement. The reason for this low pull-out force is illustrated in figure 10. Here, the equivalent plastic strain in the aluminium adaptor is shown as the axial displacement is applied. At an axial displacement of 2.24 mm, the fitting has squeezed material against the lowest point of the crimp indentation in the tube and the reaction force has risen to 6.46 kN. As the fitting is pulled further, this trapped material is pushed through the space between the tube and fitting. At a displacement of 6.56 mm, the material is fully plastic and the maximum force is reached. The pull-out load is therefore dominated by the force required to extrude this low strength aluminium. This point is further emphasised by figure 11 comparing the radial displacement of the fitting at the pull-out load for the small fitting in the large tube (with the adaptor) and the large fitting in the large tube. The deformation of the large fitting is 90 times greater than the deformation of the small fitting. This is due to the aluminium adaptor absorbing most of the deformation required to move past the indentations in the tube.

Assembly	Pull out force (kN)		
	Quarter model	Predicted total	Required
Small fitting in large tube	6.77	27.08	41.63
Large fitting in large tube	15.31	61.24	41.63
Small fitting in small tube	14.33	57.32	22.08

Table 5. Predicted axial load capacity

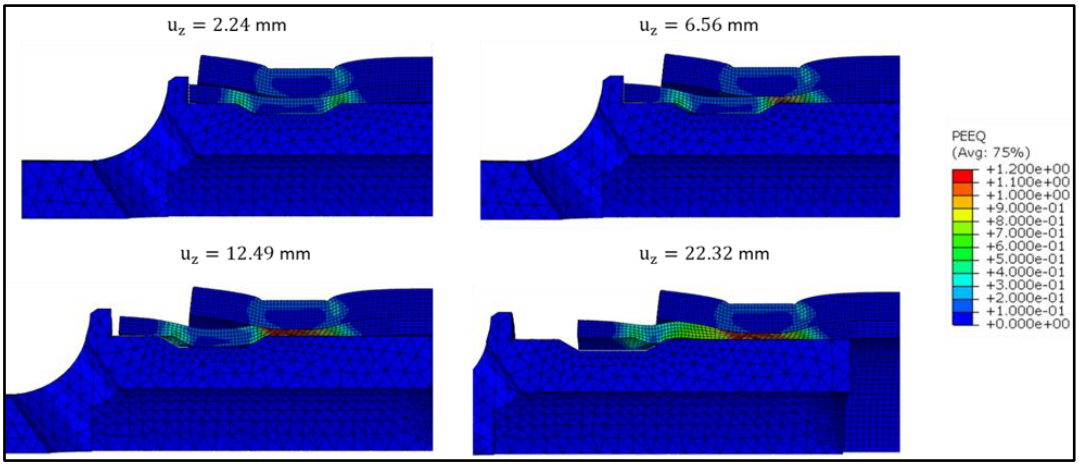

Figure 10: Equivalent plastic strain during pull-out (small fitting in large tube)

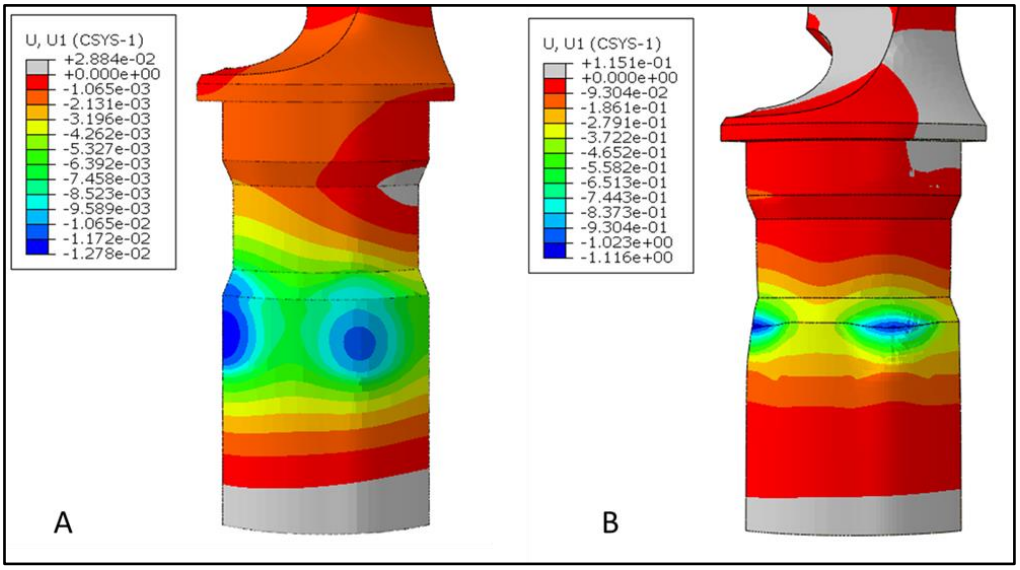

Figure 11: Radial displacement (mm) of A: small fitting in large tube and B: large fitting in large tube at peak load

3 Experimental Validation

An initial test was carried out with a small cast iron fitting and aluminium adaptor crimped in a 400 mm length of large tube. This arrangement was loaded into an Instron tensile test machine, as shown in figure 12. Displacement was applied to the pin at a rate of 0.25 mm/s. The peak load sustained by the assembly was 21.2 kN which was

approximately half the required force (see table 5). The development of load as displacement was applied is shown in figure 13, along with the loads predicted by the FEA model with a coefficient of friction of 0.1 and with no friction applied.

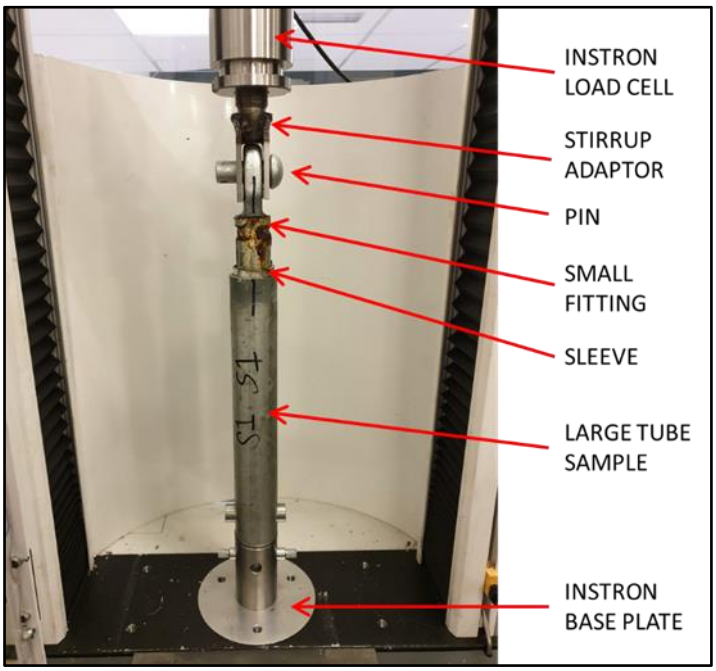

Figure 12: Test arrangement for small fitting in large tube

In figure 13 the experimental results lie between the two numerical predictions. Initially the numerical results show a stiffer assembly than the experimental results. This is due to compliance within the experimental load train. After this point a similar plateau is seen where the aluminium adaptor is being extruded. However, the numerical prediction does not show the rapid drop off in load after 10 mm of displacement. This is most likely due to the adaptor material model not being sophisticated enough to track localised material failure.

The state of the assembly following the test is shown in figure 14. As predicted by the FEA, the adaptor was partially pulled from the tube. However, ultimate failure was due to the fitting being pulled from the adaptor. The tube was split along its length in order to remove the adaptor without causing further damage. Regions where the adaptor material has been damaged, corresponding to the crimp indentations in the tube can be seen.

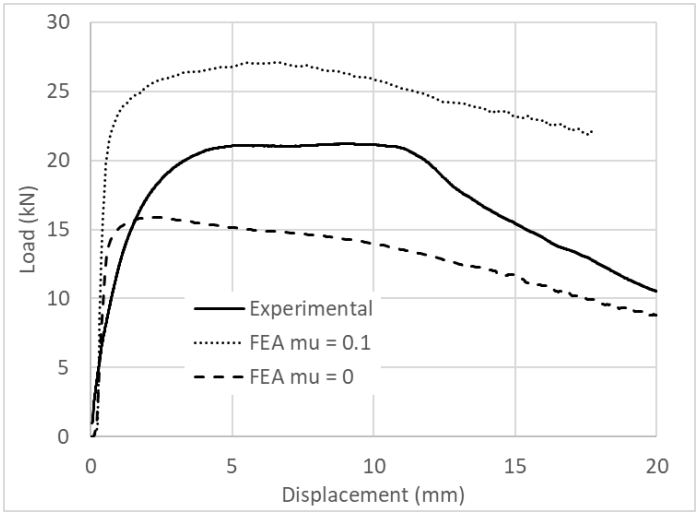

Figure 13: Predicted and measured pull-out force: small fitting in large tube

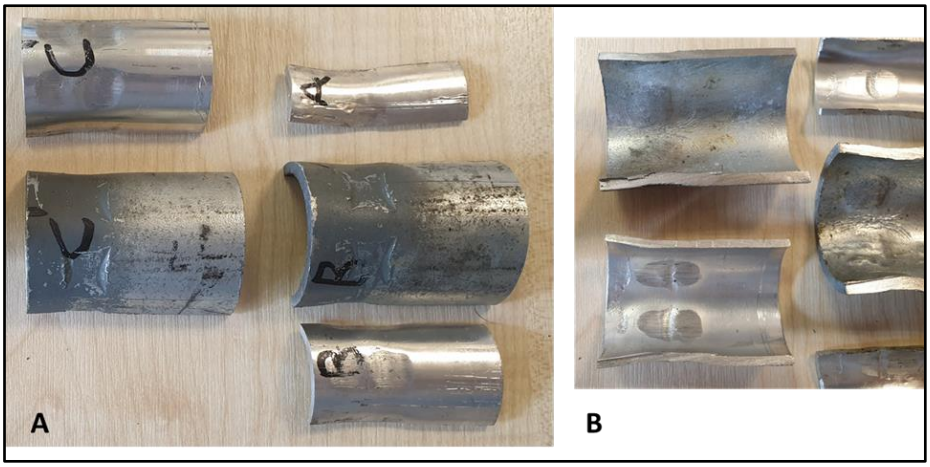

Figure 14: Large tube and adaptor following pull out test with small fitting showing outer surfaces (A) and inner surfaces (B)

Noting that the predicted pull-out force of the small fitting in the small tube was close to the 50 kN load capacity of the Instron test machine, further testing was carried out using a single actuator on the Huddersfield Adhesion and Rolling Contact Dynamics (HAROLD) test rig [11]. Again, test assemblies were made up from 400 mm lengths of tube. These were placed between the bed of the test rig and a clevis attached to the actuator. Displacement was applied at a rate of 0.4 mm/s. For each size of tube, 5 tests were carried out.

The test results are summarized in table 6. Comparing these results with the predicted and required values shown in table 5 the fittings are exceeding the design requirement and giving a higher than predicted failure load.

Figure 15 shows the FEA predicted and experimental force – displacement relationship for the small fitting in the small tube with coefficients of friction of 0, 0.1 and 0.2. Included in this figure is the measured behaviour for the samples with the smallest and largest peak pull-out load. The experimental displacement measurements include compliance in all other components in the load train whereas the FEA results

assume rigid connections at the end of the tube and at the pin. This has resulted in the experimental behaviour appearing to be less stiff as load is increased and other components in the load train extend. However, as this extension is mainly elastic, once load starts to fall, these components contract making the fitting to tube interaction appear stiffer, as extension here is absorbed by contraction of other parts of the load string. Taking this into account, there is good agreement between the numerical and experimental results. The range of peak loads predicted using coefficients of friction or 0.1 and 0.2 gives a good indication of the experimental variability.

Assembly	Experimental			Required
	Max	Min	Average	
Large fitting in large tube	62.4	49.65	54.57	41.63
Small fitting in small tube	74.67	53.7	62.46	22.08

Table 6. Axial pull-out force (kN)

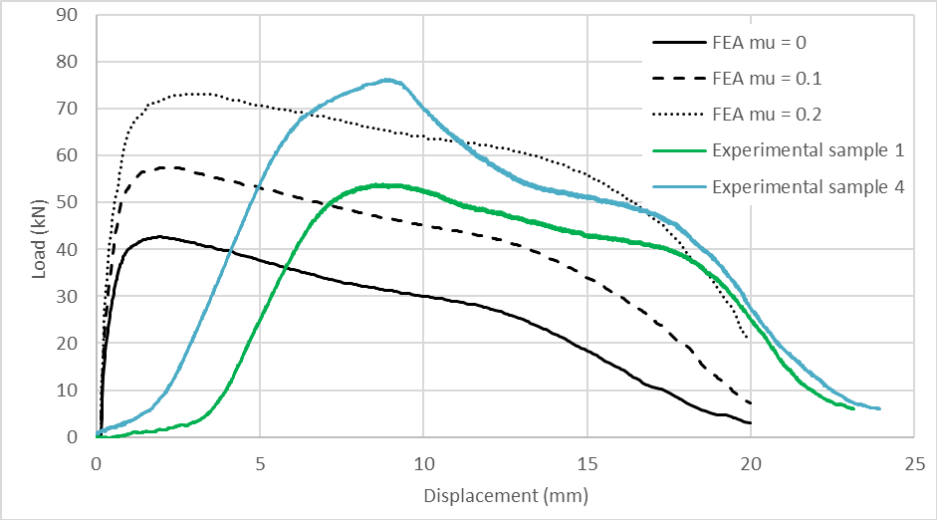

Figure 15: Predicted and measured pull-out force: small fitting in small tube

3 Conclusions

In order to meet future demands for rail electrification whilst maintaining current infrastructure, there is a need for reliable replacement parts.

Designs for parts on older sections of infrastructure were generated without the benefit of design simulation. This has resulted in some, perhaps, inappropriate design decisions. An example has been observed of the crimping of a tongue compression end fitting in a cantilever assembly failing in service.

Large and small tongue compression end fittings have been designed. These are machined from structural steel and replace the existing cast-iron fitting.

Simulation of the crimping and pull out of a tongue compression fitting in a steel tube has been carried out. This simulation used a quad-linear material model for the steel tube and new fittings. Simulations demonstrated that for both the small fitting in the small tube and the large fitting in the large tube, the required axial load capacity was

exceeded. However, for an assembly comprising a small fitting in a large tube with an adaptor, the pull-out strength was below the required level. This latter assembly failed due to the aluminium adaptor being extruded between the fitting and the tube.
Simulation has demonstrated that friction between parts in the assembly can have a substantial impact on the pull-out load. For the small fitting in the small tube, increasing the coefficient of friction from 0 to 0.2 increased the pull out load by a factor of 1.7.
The simulation was validated with a series of experimental tests. Good correlation between simulation and experiment was observed in terms of: ultimate pull-out load, pull-out load profile and material deformation. Using a coefficient of friction ranging from 0.1 to 0.2 gave a good indication of the range of the experimental variability.
Experimental testing demonstrated that using a small fitting in a large tube with an aluminium adaptor gave a load capacity which was only 52% of the design requirement.

Acknowledgements

The authors are grateful to Mr. B Bryce, for assistance in using the HAROLD rig and to Mr G Jones for proofreading this paper. The research reported in this paper was facilitated by Knowledge Transfer Program project KTP010705, funded by Innovate UK.

References

[1] Rail accident investigation branch, “Collapse of the overhead line near to Jewellery Quarter Tram Stop, Midland Metro 20 April 2011”, Department for Transport, Report 21/2012, 2012.
[2] Rail accident investigation branch, “Accident involving a pantograph and the overhead line near Littleport, Cambridgeshire 5 January 2012”, Department for Transport, Report 06/2013 v2, 2013.
[3] Network Rail, “Compression jointing of end fittings”, NR/OLE D11 issue 1, 2005.
[4] Railtrack, Drawing number UK1/142/100 issue 4, 2000.
[5] British Railways Board, Drawing number UK1/142/17/A4, 1975.
[6] BS EN 10210-1:2006
[7] Yun X, Gardner L, “Stress-strain curves for hot-rolled steels”, Journal of Constructional Steel Research, 133, 36–46, 2017.
[8] Balfour Beatty Power Construction Limited, Drawing number 142/16, 1966.
[9] AZO Materials, “Aluminium: Specifications, Properties, Classifications and Classes”, 2005. https://www.azom.com/article.aspx?ArticleID=2863, accessed 4/1/2022.
[10] Dassault Systemes. “Choosing an appropriate element”, SIMULIA User Assistance, 2021.
[11] Boyacioglu P, Bevan A, Allen P, Bryce B, Foulkes S, “Wheel Wear Performance Assessment and Model Validation Using HAROLD Full Scale Test Rig”, Proceedings of the Institution of Mechanical Engineers, Part F: Journal of Rail and Rapid Transit. 2021.